Published in final edited form as:
Biochemistry. 2011 November 1; 50(43): 9255–9263. doi:10.1021/bi201003a.

Electron Transfer Within Nitrogenase: Evidence for a Deficit-Spending Mechanism†

Karamatullah Danyal[§], **Dennis R. Dean**[#], **Brian M. Hoffman**[♠,*], and **Lance C. Seefeldt**[§,*]

[§]Department of Chemistry and Biochemistry, Utah State University, Logan Utah 84322

[#]Department of Biochemistry, Virginia Tech University, Blacksburg, Virginia 24061

[♠]Department of Chemistry, Northwestern University, Evanston, Illinois 60208.

Abstract

The reduction of substrates catalyzed by nitrogenase utilizes an electron transfer (ET) chain comprised of three metalloclusters distributed between the two component proteins, designated as the Fe protein and the MoFe protein. The flow of electrons through these three metalloclusters involves ET from the [4Fe-4S] cluster located within the Fe protein to an [8Fe-7S] cluster, called the P cluster, located within the MoFe protein and ET from the P cluster to the active site [7Fe-9S-X-Mo-homocitrate] cluster called FeMo-cofactor, also located within the MoFe protein. The order of these two electron transfer events, the relevant oxidation states of the P-cluster, and the role(s) of ATP, which is obligatory for ET, remain unknown. In the present work, the electron transfer process was examined by stopped-flow spectrophotometry using the wild-type MoFe protein and two variant MoFe proteins, one having the α-188^{Ser} residue substituted by cysteine and the other having the ß-153^{Cys} residue deleted. The data support a “deficit-spending” model of electron transfer where the first event (rate constant 168 s^{-1}) is ET from the P cluster to FeMo-cofactor and the second, 'backfill', event is fast ET (rate constant >1700 s^{-1}) from the Fe protein [4Fe-4S] cluster to the oxidized P cluster. Changes in osmotic pressure reveal that the first electron transfer is conformationally gated, whereas the second is not. The data for the ß-153^{Cys} deletion MoFe protein variant provide an argument against an alternative two-step ‘hopping’ ET model that reverses the two ET steps, with the Fe protein first transferring an electron to the P cluster, which in turn transfers an electron to FeMo-cofactor. The roles for ATP binding and hydrolysis in controlling the ET reactions were examined using ßγ-methylene-ATP as a prehydrolysis ATP analog and ADP + AlF_4^- as a post-hydrolysis analog (a mimic of ADP + P_i).

Keywords

Electron transfer; nitrogen fixation; FeS cluster; ATP hydrolysis

The reduction of N_2 to two ammonia molecules by nitrogenase requires eight electrons and eight protons, with two of the electrons and protons resulting in one H_2 formed for each N_2 reduced (eqn 1) (*1*).

$$N_2 + 8\ e^- + 8\ H^+ + 16\ MgATP \rightarrow 2\ NH_3 + H_2 + 16\ MgADP + 16\ Pi \quad \text{(eqn 1)}$$

†This work was supported by grants from the NIH (R01-GM59087 to LCS and DRD and HL 62302 to BMH).

[*]*Corresponding authors*: Lance C. Seefeldt, Chemistry and Biochemistry Department, Utah State University, 0300 Old Main Hill, Logan, UT 84322, lance.seefeldt@usu.edu, phone: 435-797-3964, fax: 435-797-3390; Brian M. Hoffman, Department of Chemistry, Northwestern University, 2145 Sheridan Road, Evanston IL 60208, bmh@northwestern.edu, phone: 847-491-3104, fax: 847-491-7713..

For the Mo-dependent nitrogenase, electrons are delivered to substrates via an electron transfer (ET) chain comprised of three metal clusters that starts at the reduced $[4Fe\text{-}4S]^{1+}$ cluster in the Fe protein (designated as F^{1+} cluster) (*2*), then goes to the [8Fe-7S] (P-cluster) in the MoFe protein, (*3, 4*) and ends on the [7Fe-9S-X-Mo-homocitrate] cluster or FeMo-cofactor (M cluster) in the MoFe protein (*5*), where substrates bind and are reduced (**Figure 1**). Transfer of a single electron to the FeMo-cofactor is initiated when the Fe protein transiently associates with the MoFe protein, with each ET event coupled to the hydrolysis of two MgATP molecules (*1*). This ET event has recently been shown to be conformationally gated (*6–8*). The order of MgATP hydrolysis and ET and the nature of their coupling remain unknown, although there is evidence to suggest that MgATP hydrolysis follows ET (*1, 6, 9, 10*). After ET and hydrolysis of MgATP, the oxidized Fe protein dissociates from the MoFe protein, enabling the MoFe protein to bind another reduced, MgATP-containing, Fe protein (*11*). This cycle must be repeated a sufficient number of times to support the reduction of the bound substrate.

At least three different models can be considered for the ATP-coupled delivery of an electron from the Fe protein to the catalytic site FeMo-cofactor. In “direct” ET, the Fe protein would reduce FeMo-cofactor directly, skipping the P cluster. The known distances and driving forces make this option theoretically possible (*12, 13*), but there are several lines of evidence against such a model, including evidence for changes in oxidation state of the P cluster during turnover (*3, 4*), and the location of the P cluster ‘in-line’ between the F and M clusters in X-ray structures of Fe protein-MoFe protein complexes (*14–16*). In a “sequential” or “hopping” model for ET, the rate-limiting step is the initial transfer of an electron from the reduced $[4Fe\text{-}4S]^{1+}$ cluster of the Fe protein (F^{1+}) to the resting state of the P cluster (P^N), generating a ‘super-reduced’ P-cluster (P^S). This initial inter-component ET step would then be followed by rapid intra-molecular ET from P^S to FeMo-cofactor (M^N), resulting in the resting P^N state and reduced FeMo-cofactor (M^R). This model is not attractive because it would require the reduction of the all ferrous P cluster (P^N) to a state (P^S) that has never been observed for the P cluster (*17, 18*). In fact, the reduction of an FeS cluster beyond the all ferrous state has never been observed for any protein (*19–22*).

A third model can be denoted “deficit-spending”. In this model, the first ET event involves the transfer of an electron from the P^N-cluster to FeMo-cofactor ($P^N \rightarrow M^N$), resulting in the formation of a P-cluster state that has been oxidized by one electron relative to the resting P^N state (P^{1+}) and reduction of the M cluster by one electron (M^R). The electron ‘deficit’ in the P-cluster is then erased by “back-fill” ET from the Fe protein to the oxidized P cluster ($F^{1+} \rightarrow P^{1+}$). This model is the most attractive of the three, being consistent with the available information, although this model has yet to be experimentally tested.

In the present work, we have conducted stopped-flow kinetic measurements of ET from the reduced Fe protein to MoFe protein of nitrogenase that test both the deficit-spending and hopping models of ET and examine the roles of ATP binding/hydrolysis and protein conformational activation in ET. Key to these studies are two MoFe protein variants with different amino acid substitutions. In one, the ß-153^{Cys} ligand to the P cluster was deleted, a change which tests aspects of the hopping model for ET. In the other, the β-188^{Ser} located in close proximity to the P cluster (**Figure 2**) was substituted by cysteine, giving a MoFe protein that contains a P cluster that exists extensively in an oxidized state (P^{1+}), (*4*). This feature was explained by a negative shift in E_m for the $P^{1+/N}$ couple (estimated to be -90 mV) that leaves P^{1+} as the majority state (~ 65%) even in the presence of the reductant dithionite, with the remaining 35 % in the P^N state. It was also suggested that E_m of the P cluster shifts because β-188^{Cys} forms a P-cluster ligand, thereby stabilizing the P^{1+} state. The availability of a catalytically competent MoFe protein whose P-cluster exhibits both P^N and P^{1+} states in the resting enzyme presented an opportunity to test the deficit-spending

model by kinetic analysis of inter-component ET from Fe protein to the substituted MoFe protein through experiments both in aqueous buffer and in solutions of varying osmotic pressure. The roles for ATP binding and hydrolysis in controlling the electron transfer reactions were examined using ßγ-methylene-ATP as a pre-hydrolysis ATP analog and ADP + AlF_4^- as a post-hydrolysis analog (a mimic of ADP + P_i).

Materials and Methods

Materials and protein purification

All reagents were obtained from Sigma-Aldrich Chemicals (St. Louis, MO). *Azotobacter vinelandii* strains DJ995 (wild-type MoFe protein), DJ1190 (β-188^{Cys} MoFe protein), DJ1193 (β-188^{Cys} MoFe protein expressed in a Δ*nifB* background, resulting in a protein lacking FeMo-cofactor, called the apo- β-188^{Cys} MoFe protein), DJ1158 (ß-$153^{deletion}$ MoFe protein), and DJ1003 (wild-type MoFe protein expressed in a Δ*nifB* background, resulting in a protein lacking FeMo-cofactor, called the apo-wild-type MoFe protein) were grown and nitrogenase MoFe proteins were expressed as described previously (*23*). All MoFe proteins contained a seven-histidine tag on the α-subunit. This allowed purification of each protein using the previously described metal affinity chromatography protocol (*23*). Based on SDS-PAGE analysis using Coomassie blue staining, all proteins were found to be greater than 95% homogeneous. The rates for proton reduction were determined using previously established protocols (*24*). The activity for wild-type MoFe was found to be ~2100 nmols H_2/min/mg MoFe protein while the activity of ß-188^{Cys} was found to be ~1200 nmols H_2/min/mg MoFe protein, similar to previously reported values (*4*). Septum sealed vials, degassed and under an argon atmosphere, were used for all manipulation of proteins. Gastight syringes were used to transfer all gasses and liquids.

Stopped-flow spectrophotometry

Electron transfer (ET) from Fe protein to MoFe protein was monitored by the increase in absorbance at 430 nm. This increase in absorbance results from the oxidation of the Fe protein [4Fe-4S] from its reduced (1+) state to its oxidized (2+) state. The change in absorbance was monitored as a function of time after mixing in a Hi-Tech SF61 stopped-flow UV-visible spectrophotometer equipped with a data acquisition and curve fitting system (Salisbury, Wilts, U.K.). The sample handling unit was kept inside an N_2-filled glovebox while the temperature of the reaction solutions was controlled using a circulating water bath kept outside the glovebox (*25*). All reactions were carried out at a temperature of 25°C, in a 100 mM HEPES buffer, pH 7.4, with 10 mM dithionite. The Fe protein and MoFe protein, when present, were contained in one drive syringe of the stopped-flow. The other drive syringe contained buffer with or without a nucleotide. The final concentrations of proteins and nucleotides were chosen to provide two Fe proteins for each MoFe protein along with excess ATP as specified in the legends to the figures. The instrument dead-time following mixing was approximately 2 ms. Earlier work showed that the absorbance increase associated with the $F^{1+} \rightarrow F^{2+}$ oxidation can be followed by slower absorbance decreases related to re-reduction of F^{2+}(*26*). As we are concerned only with the F^{1+} oxidation step, the overall time-course of a stopped-flow trace was fit to the equation for a first-order sequential reaction corresponding to $F^{1+} \rightarrow F^{2+} \rightarrow F^{1+}$ reaction; we report only the observed rate constant, k_{obs}, for the $F^{1+} \rightarrow F^{2+}$ step, as the follow-up reaction involves multiple processes, including dissociation of the Fe-MoFe protein complex. The fits to this kinetic scheme were carried out in Sigmaplot (Systat Software Inc, San Jose, CA). Osmotic pressure effects on the ET rate were examined as described (*6*).

Results

ET from Fe protein to MoFe protein

Pre-steady state ET from the Fe protein to the resting-state MoFe protein is monitored through measurement of the increase in the absorbance at 430 nm that accompanies the oxidation of F^{1+} to F^{2+} (*27, 28*). Stopped-flow mixing of reduced Fe protein with wild-type resting-state MoFe protein in the presence of saturating MgATP yields stoichiometric oxidation of F^{1+} (**Figure 3**) in a process that is exponential, with a rate constant, k_{obs} = 168 s^{-1}, that is consistent with earlier studies (*26*).

When the ß-188^{Cys} MoFe protein is mixed with reduced Fe protein plus MgATP, the absorbance change indicates that ET associated with oxidation of F^{1+} also is stoichiometric (**Figure 3**). However, unlike reaction with the wild-type MoFe protein, the Fe protein oxidation by ß-188^{Cys} MoFe protein shows an ET "burst", with ~ 65 % of the F^{1+} oxidation occurring during the instrument dead-time (2 ms). The remaining 35% oxidation occurs with a resolved time-course that can be fit to an exponential with a rate constant k_{obs} = 187 s^{-1}, essentially the same as observed for the wild-type MoFe protein (*25*). The ß-188^{Cys} MoFe protein in dithionite solution was earlier shown to exist as an equilibrium mixture of 3 states of the P cluster (P^{1+}, P^{2+}, and P^{N}), with the total contribution from the two oxidized forms, being ~ 65 % of the enzyme present with ~ 35 % existing as the resting oxidation state, P^{N} (*4*). The kinetically resolved phase of the stopped-flow trace, with rate constant equivalent to that for wild-type MoFe protein, is thus assigned to oxidation of F^{1+} by ß-188^{Cys} MoFe protein in the P^{N}/M^{N} state, with the "burst" ET phase being assigned to rapid oxidation of F^{1+} by P^{1+} of the ß-188^{Cys} MoFe protein in the P^{1+}/M^{N} state. This assignment is confirmed below.

In a separate study, when the ß-153^{Cys} of the MoFe protein was deleted, this MoFe protein variant showed stoichiometric oxidation of F^{1+} with a rate constant essentially unchanged from that observed to the wild-type MoFe protein.

The roles of nucleotides in ET

We next consider the contributions of nucleotides to the ET events to the ß-188^{Cys} MoFe protein. Both the binding and hydrolysis of ATP within the Fe protein is intimately linked to ET from the Fe protein to the wild-type MoFe protein during substrate reduction. MgADP and MgATP analogs do not support the ET reaction (*29*). As shown in **Figure 3**, MgADP also does not support oxidation of the Fe protein by the ß-188^{Cys} MoFe protein: neither the burst nor the resolved kinetic phases are observed. Thus, it can be concluded that MgATP binding, at a minimum, is required for both the burst-phase reduction of P^{1+} of the ß-188^{Cys} MoFe protein in the P^{1+}/M^{N} state as well as the resolved ET to the P^{N}/M^{N} state.

To further differentiate the respective roles of ATP binding and hydrolysis in ET from the Fe protein to the ß-188^{Cys} MoFe protein, ET reactions were monitored in the presence of ATP analogs. The complex between Fe protein and MoFe protein that contains the non-hydrolyzable analog βγ-methylene-ATP was earlier shown to induce conformational changes in the Fe protein similar to those induced by MgATP, yet the analog is not hydrolyzed by nitrogenase (*30–33*). As previously reported (*30*), βγ-methylene-ATP does not support ET from the Fe protein to the wild-type MoFe (**Figure 4**). Likewise, this analog does not support the resolved phase of Fe protein oxidation by the ß-188^{Cys} MoFe protein. However, this ATP analog does support the burst ET from the Fe protein to P^{1+}. Thus, the conformational changes in the Fe protein and/or in the Fe protein-MoFe protein complex induced by binding of βγ-methylene-ATP are sufficient to enable the rapid $F^{1+} \rightarrow P^{1+}$ ET, but not the ET from $F^{1+}$to the MoFe protein in the P^{N}/M^{N} state.

It has been proposed for several ATP-hydrolyzing enzymes (*34*, *35*), including nitrogenase, that the state following ATP hydrolysis, but before Pi release, [MoFe-Fe(2MgADP + 2 Pi)], is simulated when MgADP + AlF_4^- is bound (*15*). In the wild-type nitrogenase, this analog induces a tight complex between the Fe protein and the MoFe protein (*15*, *36*). This complex does not exhibit the normal Fe protein oxidation, only very slow ET from Fe protein to MoFe protein. In agreement with this, we observe no ET over the normal observation times (0.5 s) for a complex that includes wild-type MoFe protein, reduced Fe protein, and this nucleotide analog (**Figure 5, panel B**). Likewise, the resolved phase of Fe protein oxidation is suppressed in the ß-188^{Cys} MoFe protein-Fe[MgADP + AlF_4^-] protein complex; however, the complex shows that the burst oxidation of the Fe protein during the mixing time is preserved (**Figure 5, panel A**). Thus, both the non-hydrolyzable ATP analog, βγ-methylene-ATP, and the analog for ADP + Pi, MgADP + AlF_4^-, promote the rapid $F^{1+} \rightarrow P^{1+}$ ET reaction, whereas neither analog supports the resolved ET from the Fe protein to either wild-type or ß-188^{Cys} MoFe protein that contains P^N.

The role of FeMo-cofactor in the ET

Electrons transferred into the MoFe protein ultimately end up on FeMo-cofactor. If the ET burst observed when β-188^{Cys} MoFe protein and Fe protein are mixed with MgATP indeed reflects ET from the Fe protein [4Fe-4S] cluster to P^{1+}, then the FeMo-cofactor should not be involved in this ET event and its absence should have no influence on the observed ET burst. To test this, we purified variants of both wild-type and β-188^{Cys} MoFe proteins that do not contain FeMo-cofactor (called apo-wild-type and apo-β-188^{Cys} MoFe proteins) (*4*, *23*). When apo-wild-type MoFe protein is used, no ET is observed (**Figure 6**). When the apo-β-188^{Cys} MoFe protein and Fe protein were mixed against MgATP, the stopped-flow trace exhibited an ET burst that was indistinguishable from that seen for the FeMo-cofactor containing β-188^{Cys} MoFe protein (**Figure 6**), while the slower, resolved phase was absent.

These observations confirm that the kinetically resolved ET represents $P^N \rightarrow M^N$ ET, whereas the burst observed for the β-188^{Cys} is $F^{1+} \rightarrow P^{1+}$ ET.

Conformationally gated ET

Recently, it was shown that the rate of ET from the Fe protein to the wild-type MoFe protein is sensitive to osmotic pressure, indicating that the rate-limiting step in the ET reaction is gated by large protein conformational changes (*6*). Changes in osmotic pressure modulate the energetics of reactions that involve conformational changes in which the number of bound waters is changed. The rate constant (k_m) for such a process varies exponentially with the molality (m) of added solute according to the equation, $k_m \propto \exp[-(\Delta n/55.6)m]$, where Δn is the number of waters absorbed in the transformation (*6*).

Repeating this experiment with β-188^{Cys} MoFe protein shows that the relative proportions of the burst and resolved ET phases are independent of the presence of sucrose as osmolyte up to a sucrose concentration of ~ 2 *m* (**Figure 7**). This indicates that the presence of the osmolyte does not alter the reduction potential of P cluster, which would alter the relative proportions of P^{1+} and P^N forms and thus the relative contributions of the two kinetic phases. Unlike the burst phase, the resolved phase of the ET is dependent on osmotic pressure. The inset to **Figure 7** shows that rate constants ($k_{obs}(m)$) for ET from Fe protein to either the wild-type MoFe protein or the resolved phase ET to the β-188^{Cys} MoFe protein have essentially identical responses to sucrose addition, with the rate constants depending exponentially on the molality (m) of added sucrose with a slope corresponding to Δn ~ + 80 waters. Taking roughly one water to be bound per ~ 10 $Å^2$ of exposed surface, Δn ~ 80 waters would correspond to a conformational transition in which ~ 800 $Å^2$ of surface becomes exposed (*6*).

The present results thus indicate that ET to the MoFe state that contains P^N and M^N is conformationally gated in both wild-type MoFe and β-188^{Cys} MoFe protein, and that the amino acid substitution of β-188^{Ser} by a cysteine does not alter the conformational gate. In contrast, the presence of sucrose osmolyte up to 2 *m* does not affect the burst ET to the point where it becomes visible after the dead-time of the instrument. These results suggest that whereas the resolved oxidation of F^{1+} by the MoFe protein in the P^N/M^N state is conformationally gated, the rapid $F^{+1}\rightarrow P^{1+}$ ET event is not.

Discussion

While a deficit-spending scheme for nitrogenase ET events is the most reasonable of the three proposed, this model has proven difficult to test experimentally. For example, until now it has not been possible to measure the contributions of the individual inter- and intra-molecular ET events postulated by this model (k_{FP} and k_{PM}, respectively, **Figure 1**, panel B) to the observed ET rate constant (k_{obs}). We discuss how the experiments described in this report support a deficit-spending model of ET in nitrogenase and further argue against a hopping ET scheme, and provide insights into the roles of nucleotides in ET. We conclude by presenting a model for the sequence of events for the entire nitrogenase ET cycle that integrates the present results with earlier findings.

ET by a deficit-spending mechanism

In the present work, the deficit spending model was addressed by using the ß-188^{Cys}-substituted MoFe protein, which has P^{1+} in the resting state (*4*). This situation offered the opportunity to directly monitor the $F^{1+}\rightarrow P^{1+}$ ET event (backfill) without the need for a prior $P^N \rightarrow M^N$ ET step. For this substituted protein, the rapid intermolecular ET event from the Fe protein to the MoFe protein could be assigned to the $F^{1+}\rightarrow P^{1+}$ ET event, which was found to be faster than the dead-time of the stopped-flow instrument with a rate constant that can be estimated $k_{FP} > 1700\ s^{-1}$. This rate constant is far greater than $k_{obs} = 168\ s^{-1}$ observed for ET from the Fe protein to MoFe protein in the P^N/M^N state, indicating that intramolecular $P^N \rightarrow M^N$ ET is the rate-limiting step.

In the ET traces for ß-188^{Cys}-substituted MoFe protein, the initial ET burst assigned to $F^{1+}\rightarrow P^{1+}$ is followed by a slower resolved ET phase. This slower phase is assigned to ET from the Fe protein to the ß-188^{Cys} MoFe protein in the P^N/M^N state., and its rate constant is the same as that observed for ET from the Fe protein to the wild-type MoFe protein in the P^N/M^N state. Thus, measurement of electron transfer using the ß-188^{Cys}-substituted MoFe protein reveals both the $F^{1+}\rightarrow P^{1+}$ ET event observed as a burst and the $P^N \rightarrow M^N$ ET event observed as a slower, resolved phase.

These observations are in full accord with expectations based on the deficit-spending model. In this model, the $P^N \rightarrow M^N$ ET event is the rate-limiting step in ET from the Fe protein to the MoFe protein, and the observed ET rate constant for the oxidation of F^{1+} by the MoFe protein in the P^N/M^N state is assigned to this event: $k_{obs} = k_{PM}$. The subsequent 'backfill' ET (k_{FP}) reaction, $F^{1+}\rightarrow P^{1+}$, does not contribute to the observed ET because it is at least 10-times faster. This sequence of ET events, with the corresponding large differences in rate constants, provides an explanation for the fact that only very low levels of a P^{1+} or P^{2+} state have been observed by electron paramagnetic resonance (EPR) spectroscopy when the nitrogenase complex is freeze-trapped during steady-state turnover (*1, 37, 38*). Although the P^{1+} state is EPR active, it cannot build up to any appreciable concentration in the deficit-spending mechanism because the rate of reduction of P^{1+} by the Fe protein ($F^{1+}\rightarrow P^{1+}$) is much faster than the rate of oxidation of P^N by M cluster ($P^N \rightarrow M^N$), resulting in mostly the P^N state (which is EPR silent) under steady-state turnover.

Gated ET

The rate constant for ET from the Fe protein to the MoFe protein (k_{obs}) is sensitive to osmotic pressure, which has been assigned to protein conformational changes that gate the intermolecular ET event (*6*). This conformational change was calculated to involve exposure of a substantial (>800 A^2) protein surface area (*6*). The present study shows no modulation of the rapid backfill ET ($F^{1+} \rightarrow P^{1+}$) by changes in osmotic pressure, suggesting that this ET step is not gated by protein conformational changes; in any case, this step is so rapid that it cannot be involved in determining the observed rate of ET. Thus, it can be concluded that the protein conformational gate for ET applies specifically to the $P^N \rightarrow M^N$ intramolecular ET step.

What conformational processes could be coupled to the $P^N \rightarrow M^N$ ET reaction? Examination of X-ray structures of various complexes of the Fe protein with the MoFe protein (with or without nucleotides bound) reveal large changes in the Fe protein-MoFe protein interface, involving changes in exposed protein surface area, but do not reveal any significant changes within the MoFe protein that could explain how the Fe protein with two bound 2ATP might activate the $P^N \rightarrow M^N$ ET (*14*). An attractive 'compound gate' model can be developed, however, from examination of the X-ray structure of an oxidized MoFe protein (P^{1+}, M^N) (*39*). From this structure, the P^{2+} cluster is stabilized by the coordination of the side-chain of ß-188^{Ser} to an Fe atom of the P cluster (*39*). We suggest that conformational activation of resting-state MoFe protein by an as-yet unidentified change in the Fe protein-MoFe protein interface could cause the ß-188^{Ser} side-chain to transiently coordinate to an Fe atom of P^N, thereby creating an activated state of the P cluster (designated P^{N*}) with a lowering of the potential to the point that $P^{N*} \rightarrow M^N$ ET becomes favorable. For the ß-188^{Cys} MoFe protein, the assumption is that a cysteine at this position shifts the equilibrium in favor of the state with the cysteinate bound to the Fe of the P cluster, and that the redox equilibrium between P^N and P^{1+} in the presence of dithionite also involves a ligation equilibrium, with ~ 65% of the P cluster in the form of P^{1+} with bound cysteine, and ~35% in the form of P^N with cysteine not bound as in the wild-type MoFe protein. This picture would account for the observation that the resolved ET phase for the ß-188_{Cys} MoFe protein behaves the same as that for the wild-type MoFe protein. Lowe and Thorneley (*26*) further treat ET as occurring only as part of the transfer of an `H-atom', namely an electron and a proton.

Two recent reports describing ET to the MoFe protein in the absence of the Fe protein also support an activation step that could facilitate the intramolecular $P^{N*} \rightarrow M^N$ ET step. It has been found that attaching a Ru-ligand complex onto the surface of the MoFe protein near the P cluster can be used to photoinduce ET from the Ru-ligand complex into the MoFe protein, allowing acetylene reduction (*40*). In the absence of the Fe protein, the rates of acetylene reduction were very low (0.2% of the rate observed with Fe protein and ATP), consistent with the need for some activation of the $P \rightarrow M$ ET process to promote full substrate reduction rates. In a separate study, it was found that a low potential Eu(II)-ligand complex could be used to drive electrons into the MoFe protein in the absence of the Fe protein in support of reduction of hydrazine ($H_2N\ NH_2$) to two ammonia (*41*). In this system, substrate reduction was observed only when an amino acid residue located between the P cluster and M cluster was substituted by another amino acid, suggesting that the conformational switch normally activated by Fe protein binding involves changes in residues located between the P cluster and FeMo-cofactor and that the key conformational changes can be partially mimicked by an amino acid substitution (*41*).

Further evidence against a hopping model

The strongest argument against a hopping or sequential ET model for nitrogenase is the improbability that the P cluster can be reduced beyond the all ferrous P^N state, as would

occur following an initial ET event: $F^{1+} \rightarrow P^N$. Super-reduction of all-ferrous P^N would require the formation of an Fe(I) with tetrahedral coordination by sulfur, an unknown Fe state. However, our results show that this step would have to be gated, and one might imagine that the activation process might involve a transient loss of a cysteinate ligand from one of the Fe atoms. This would create an activated $P^{N\dagger}$ cluster state that has a three-coordinate Fe(II) and a more positive reduction potential. Such a state might accept an electron from F^{1+}, and then re-binding of the cysteinate could create a strongly reducing P^S state that undergoes prompt follow-up $P^S \rightarrow M^N$ ET.

To test this possibility, we examined ET from F^{1+} to a MoFe protein where one of the cysteine ligands to the P cluster was removed (ß-$153^{Cys}\Delta$). It was found that the rate of oxidation of F^{1+} to this MoFe protein variant is unchanged from the rate to the wild-type MoFe protein, providing further evidence against the hopping ET model.

Role for nucleotides

MgATP binding and hydrolysis are both essential to intermolecular ET from the Fe protein to the MoFe protein (*42*). In the absence of ATP hydrolysis, the Fe protein does not transfer an electron to the resting-state MoFe protein (P^N, M^N). The role of ATP hydrolysis in this ET process cannot be filled by the non-hydrolyzable ATP analog ßγ-CH_2-ATP or the ADP +Pi analog, ADP-AlF_4. However, results reported here reveal that ATP hydrolysis is not necessary for the backfill ET ($F^{1+} \rightarrow P^{1+}$). Rather, the burst ET to the β-188^{Cys} MoFe protein is supported by both ßγ-CH_2-ATP and ADP-AlF_4. Thus, the backfill electron transfer event ($F^{1+} \rightarrow P^{1+}$) is not conformationally gated and requires nucleotide binding but not hydrolysis.

In contrast to this finding, neither of the ATP analogs supported the slower, resolved phase ET assigned to the $P^N \rightarrow M^N$ ET reaction, pointing to this ET step as requiring an ATP-bound state that has not yet been achieved. Both MgATP and MgADP binding to the Fe protein have been shown to equally lower the midpoint reduction potential of the $[4Fe\text{-}4S]^{2+/1+}$ couple (*33*), yet MgADP does not support either the $P^N \rightarrow M^N$ or the $F^{1+} \rightarrow P^{1+}$ ET events, revealing that it is not simply an issue of driving force for the ET. Thus, the studies presented here pinpoint *(i)* the conformational gate and *(ii)* the specific need for ATP binding/hydrolysis to the $P^N \rightarrow M^N$ ET step.

Summary sequence of events

The findings presented here, taken with earlier findings, can be used to propose an overall model for the events associated with ET from the Fe protein to the MoFe protein (**Figure 8**). In this model, the ET process is initiated by the association of the Fe protein (2MgATP) with the resting state of the MoFe protein (**Figure 8**, step 1). Although the binding of 2 MgATP to the Fe protein causes a major structural change and lowers its reduction potential by -120 mV (*43*), the osmotic pressure dependence of the oxidation of F^{1+} indicates that the complex initially formed between Fe protein-2MgATP and MoFe protein is not competent for ET (*6*). Instead, ET is initiated by a conformational activation (**Figure 8**, step 2), presumably involving motion at the Fe protein-MoFe protein interface, with exposure of as many as ~80 water molecules (*6*). In this model, the interface motion is coupled to a conformational change (second gate) (**Figure 8**, step 3) within the MoFe protein that shifts the P cluster to an activated state (P^{N*}) that that transiently favors intramolecular ET from the P^{N*} state to the M^N cluster (**Figure 8**, step 4) (*6*). The final step in this sequence involves the rapid 'backfill' ET to the oxidized P cluster ($F^{1+} \rightarrow P^{1+}$), resulting in an oxidized Fe protein and a reduced MoFe protein that has its metal clusters in the P^N and M^R states (**Figure 8**, step 5).

The specific contributions for MgATP binding and hydrolysis to the individual steps remains to be resolved, but our studies show that the backfill ET process requires nucleotide binding but not hydrolysis, while the activated $P^{N*} \rightarrow M^{N}$ ET initial step is not facilitated by any of the ATP analogs examined, requiring ATP itself. Studies of a wide range of ATP utilizing enzymes, in particular transport proteins, have led to the general view that energy transduction in these proteins occurs during the binding of MgATP, which induces a conformational state activated for the particular function of the ATPase ('taut' state). ATP hydrolysis occurs after the functional/catalytic step, initiating relaxation from the taut state to a relaxed state with ADP bound, which in turn leads to a resetting of the system for another round of catalysis (*34, 35*).

While the order of ET and MgATP hydrolysis in nitrogenase has not been well established by previous work, the consensus model is that MgATP hydrolysis follows the ET events (*1, 44, 45*), in agreement with the current views of ATPase function in other proteins. MgATP binding to the Fe protein is known to induce protein conformational changes that increase the affinity of the Fe protein for binding to the MoFe protein, but given that further activation is needed to induce ET, it would appear that conversion to some as yet uncharacterized ATP binding state (perhaps a true transition state) is required to activate the $P^{N} \rightarrow M^{N}$ ET. In this model, the MgATP hydrolysis reaction is placed late in the reaction, after all ET events, although as just noted, this order has not been clearly resolved (**Figure 8**, step 6). The present results reveal that the backfill ET from $F^{+1} \rightarrow P^{1+}$ requires an ATP-bound state, but does not require ATP hydrolysis. It thus seems reasonable to suggest that nitrogenase functions similarly to other ATPases, and that ATP hydrolysis during nitrogenase ET is a late event that relaxes the Fe protein for dissociation from the MoFe protein. The rate limiting step for the overall reduction of substrates has been shown to be dissociation of the oxidized Fe protein with two bound 2MgADP from the MoFe protein (**Figure 8**, step 7), with a rate constant of ~ 6 s^{-1} (*26*).

Abbreviations

Fe protein	iron protein of nitrogenase
MoFe protein	molybdenum-iron protein of nitrogenase
FeMo-cofactor	iron-molybdenum cofactor
M cluster	iron-molybdenum cofactor
F cluster	[4Fe-4S] cluster of the Fe protein
P cluster	[8Fe-7S] cluster of the MoFe protein
ET	electron transfer

References

1. Burgess BK, Lowe DJ. Mechanism of molybdenum nitrogenase. Chem. Rev. 1996; 96:2983–3012. [PubMed: 11848849]
2. Georgiadis MM, Komiya H, Chakrabarti P, Woo D, Kornuc JJ, Rees DC. Crystallographic structure of the nitrogenase iron protein from *Azotobacter vinelandii*. Science. 1992; 257:1653–1659. [PubMed: 1529353]
3. Lowe D, Fisher K, Pau R, Thorneley R. Kinetics and mechanism of nitrogenase - a role for P centers in dinitrogen reduction. Curr. Plant Sci. Biotech. Agricul. 1993; 17:95–100.
4. Chan JM, Christiansen J, Dean DR, Seefeldt LC. Spectroscopic evidence for changes in the redox state of the nitrogenase P-cluster during turnover. Biochemistry. 1999; 38:5779–5785. [PubMed: 10231529]

5. Chan MK, Kim J, Rees DC. The nitrogenase FeMo-cofactor and P-cluster pair: 2.2 Å resolution structures. Science. 1993; 260:792–794. [PubMed: 8484118]
6. Danyal K, Mayweather D, Dean DR, Seefeldt LC, Hoffman BM. Conformational gating of electron transfer from the nitrogenase Fe protein to MoFe protein. J. Am. Chem. Soc. 2010; 132:6894–6895. [PubMed: 20429505]
7. Davidson VL. Protein control of true, gated, and coupled electron transfer reactions. Acc. Chem. Res. 2008; 41:730–738.
8. Hoffman BM, Ratner MA. Gated electron transfer: when are observed rates controlled by conformational interconversion? J. Am. Chem. Soc. 1987; 109:6237–6243.
9. Mensink RE, Haaker H. Temperature effects on the MgATP-induced electron transfer between the nitrogenase proteins from *Azotobacter vinelandii*. Eur. J. Biochem. 1992; 208:295–299. [PubMed: 1521527]
10. Thorneley RN, Ashby G, Howarth JV, Millar NC, Gutfreund H. A transient-kinetic study of the nitrogenase of *Klebsiella pneumoniae* by stopped-flow calorimetry. Comparison with the myosin ATPase. Biochem. J. 1989; 264:657–661. [PubMed: 2695063]
11. Hageman RV, Burris RH. Nitrogenase and nitrogenase reductase associate and dissociate with each catalytic cycle. Proc. Natl. Acad. Sci. U.S.A. 1978; 75:2699–2702. [PubMed: 275837]
12. Edwards PP, Gray HB, Lodge MTJ, Williams RJP. Electron transfer and electronic conduction through an intervening medium. Angew. Chem. Int. Ed. Engl. 2008; 47:6758–6765. [PubMed: 18651676]
13. Gray HB, Winkler JR. Electron flow through metalloproteins. Biochim. Biophys. Acta. 2010; 1797:1563–1572. [PubMed: 20460102]
14. Tezcan FA, Kaiser JT, Mustafi D, Walton MY, Howard JB, Rees DC. Nitrogenase complexes: multiple docking sites for a nucleotide switch protein. Science. 2005; 309:1377–1380. [PubMed: 16123301]
15. Schindelin H, Kisker C, Schlessman JL, Howard JB, Rees DC. Structure of ADP x $AlF_4^{(-)}$-stabilized nitrogenase complex and its implications for signal transduction. Nature. 1997; 387:370–376. [PubMed: 9163420]
16. Chiu H, Peters JW, Lanzilotta WN, Ryle MJ, Seefeldt LC, Howard JB, Rees DC. MgATP-Bound and nucleotide-free structures of a nitrogenase protein complex between the Leu 127 Delta-Fe-protein and the MoFe-protein. Biochemistry. 2001; 40:641–650. [PubMed: 11170380]
17. Yoo SJ, Angove HC, Papaefthymiou V, Burgess BK, Münck E. Mössbauer study of the MoFe protein of nitrogenase from *Azotobacter vinelandii* using selective ^{57}Fe enrichment of the M-centers. J. Am. Chem. Soc. 2000; 122:4926–4936.
18. Lindahl PA, Papaefthymiou V, Orme-Johnson WH, Münck E. Mössbauer studies of solid thionin-oxidized MoFe protein of nitrogenase. J. Biol. Chem. 1988; 263:19412–19418. [PubMed: 2848826]
19. Mouesca J-M, Noodleman L, Case DA. Analysis of the ^{57}Fe hyperfine coupling constants and spin states in nitrogenase P-clusters. Inorg. Chem. 1994; 33:4819–4830.
20. Surerus KK, Hendrich MP, Christie PD, Rottgardt D, Orme-Johnson WH, Münck E. Mössbauer and integer-spin EPR of the oxidized P-clusters of nitrogenase: POX is a non-Kramers system with a nearly degenerate ground doublet. J. Am. Chem. Soc. 1992; 114:8579–8590.
21. Angove HC, Yoo SJ, Münck E, Burgess BK. An all-ferrous state of the Fe protein of nitrogenase. Interaction with nucleotides and electron transfer to the MoFe protein. J. Biol. Chem. 1998; 273:26330–26337. [PubMed: 9756863]
22. Chakrabarti M, Deng L, Holm RH, Münck E, Bominaar EL. The modular nature of all-ferrous edge-bridged double cubanes. Inorg Chem. 2010; 49:1647–1650. [PubMed: 20073485]
23. Christiansen J, Goodwin PJ, Lanzilotta WN, Seefeldt LC, Dean DR. Catalytic and biophysical properties of a nitrogenase Apo-MoFe protein produced by a nifB-deletion mutant of *Azotobacter vinelandii*. Biochemistry. 1998; 37:12611–12623. [PubMed: 9730834]
24. Barney BM, Igarashi RY, Dos Santos PC, Dean DR, Seefeldt LC. Substrate interaction at an iron-sulfur face of the FeMo-cofactor during nitrogenase catalysis. J. Biol. Chem. 2004; 279:53621–53624. [PubMed: 15465817]

25. Lanzilotta WN, Fisher K, Seefeldt LC. Evidence for electron transfer from the nitrogenase iron protein to the molybdenum-iron protein without MgATP hydrolysis: characterization of a tight protein-protein complex. Biochemistry. 1996; 35:7188–7196. [PubMed: 8679547]
26. Thorneley, R.; Lowe, D. Molybdenum Enzymes. Wiley-Interscience Publications; New York: 1985. Kinetics and mechanism of the nitrogenase enzyme; p. 221-284.
27. Thorneley RN. Nitrogenase of *Klebsiella pneumoniae*. A stopped-flow study of magnesium-adenosine triphosphate-induce electron transfer between the component proteins. Biochem. J. 1975; 145:391–396. [PubMed: 1098654]
28. Thorneley RN, Lowe DJ. The mechanism of *Klebsiella pneumoniae* nitrogenase action. Pre-steady-state kinetics of an enzyme-bound intermediate in N_2 reduction and of NH_3 formation. Biochem. J. 1984; 224:887–894. [PubMed: 6395862]
29. Thorneley RN, Lowe DJ, Eday RR, Miller RW. The coupling of electron transfer in nitrogenase to the hydrolysis of magnesium adenosine triphosphate. Biochem. Soc. Trans. 1979; 7:633–636. [PubMed: 383544]
30. Weston MF, Kotake S, Davis LC. Interaction of nitrogenase with nucleotide analogs of ATP and ADP and the effect of metal ions on ADP inhibition. Arch. Biochem. Biophys. 1983; 225:809–817. [PubMed: 6354096]
31. Lanzilotta WN, Holz RC, Seefeldt LC. Proton NMR investigation of the $[4Fe\text{--}4S]^{1+}$ cluster environment of nitrogenase iron protein from *Azotobacter vinelandii*: defining nucleotide-induced conformational changes. Biochemistry. 1995; 34:15646–15653. [PubMed: 7495793]
32. Meyer J, Gaillard J, Moulis JM. Hydrogen-1 nuclear magnetic resonance of the nitrogenase iron protein (Cp2) from *Clostridium pasteurianum*. Biochemistry. 1988; 27:6150–6156. [PubMed: 2847787]
33. Zumft WG, Palmer G, Mortenson LE. Electron paramagnetic resonance studies on nitrogenase. II. Interaction of adenosine 5'-triphosphate with azoferredoxin. Biochim. Biophys. Acta. 1973; 292:413–421. [PubMed: 4349919]
34. Locher KP. Structure and mechanism of ATP-binding cassette transporters. Phil. Trans. Royal Soc. B. 2009; 364:239–245.
35. Linton K, Higgins C. Structure and function of ABC transporters: the ATP switch provides flexible control. Plugers Archiv. Eur. J. Phys. 2007; 453:555–567.
36. Duyvis MG, Wassink H, Haaker H. Formation and characterization of a transition state complex of *Azotobacter vinelandii* nitrogenase. FEBS Lett. 1996; 380:233–236. [PubMed: 8601431]
37. Lowe DJ, Fisher K, Thorneley RN. *Klebsiella pneumoniae* nitrogenase: pre-steady-state absorbance changes show that redox changes occur in the MoFe protein that depend on substrate and component protein ratio; a role for P-centres in reducing dinitrogen? Biochem. J. 1993; 292:93–98. [PubMed: 8389132]
38. Cameron LM, Hales BJ. Investigation of CO binding and release from Monitrogenase during catalytic turnover. Biochemistry. 1998; 37:9449–9456. [PubMed: 9649328]
39. Peters JW, Stowell MH, Soltis SM, Finnegan MG, Johnson MK, Rees DC. Redox-dependent structural changes in the nitrogenase P-cluster. Biochemistry. 1997; 36:1181–1187. [PubMed: 9063865]
40. Roth LE, Nguyen JC, Tezcan FA. ATP- and iron–protein-independent activation of nitrogenase catalysis by light. J. Am. Chem. Soc. 2010; 132:13672–13674. [PubMed: 20843032]
41. Danyal K, Inglet BS, Vincent KA, Barney BM, Hoffman BM, Armstrong FA, Dean DR, Seefeldt LC. Uncoupling nitrogenase: catalytic reduction of hydrazine to ammonia by a MoFe protein in the absence of Fe protein-ATP. J. Am. Chem. Soc. 2010; 132:13197–13199. [PubMed: 20812745]
42. Howard JB, Rees DC. Nitrogenase: a nucleotide-dependent molecular switch. Annu. Rev. Biochem. 1994; 63:235–264. [PubMed: 7979238]
43. Lanzilotta WN, Seefeldt LC. Changes in the midpoint potentials of the nitrogenase metal centers as a result of iron protein-molybdenum-iron protein complex formation. Biochemistry. 1997; 36:12976–12983. [PubMed: 9335558]
44. Mensink RE, Wassink H, Haaker H. A reinvestigation of the pre-steady-state ATPase activity of the nitrogenase from *Azotobacter vinelandii*. Eur. J. Biochem. 1992; 208:289–294. [PubMed: 1325902]

45. Lowe, D.; Ashby, G.; Brune, M.; Knights, H.; Webb, M.; Thorneley, R. Nitrogen Fixation: Fundamentals and Applications. Kluwer Academic Publishers; St. Petersburg, Russia: 1995. ATP hydrolysis and energy transduction by nitrogenase; p. 103-108.

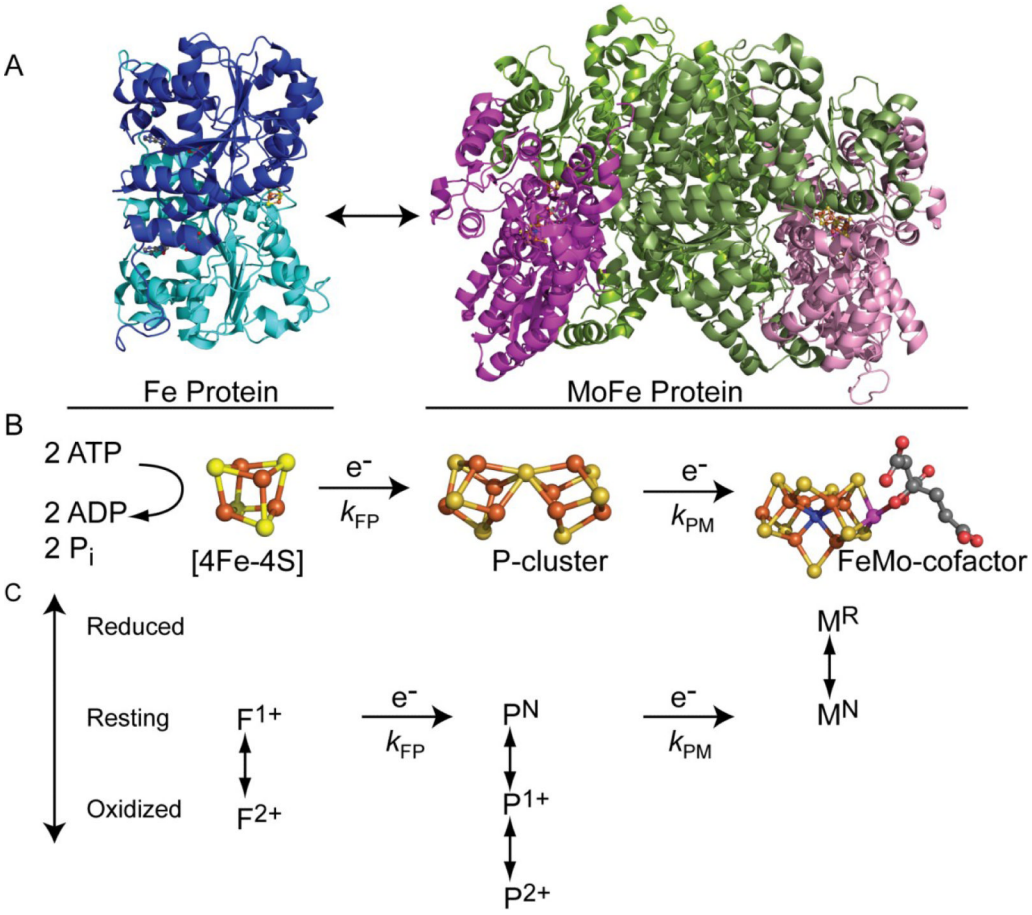

Figure 1. Nitrogenase proteins and electron transfer between metal clusters

(**Panel A**) The Fe protein (left) is shown docking to an αγ-unit of the MoFe protein (right). (**Panel B**) The two electron transfer steps: from the Fe protein [4Fe-4S] cluster (F) to the MoFe protein P cluster (P) (k_{FP}) and from the P cluster (P) to the FeMo-cofactor (M) (k_{PM}). Two ATP are hydrolyzed to two ADP and two Pi during each docking event. (**Panel C**) The relevant oxidation states of the three metal cluster are shown, with the resting state (in the presence of dithionite) shown in the middle, and more reduced states shown going up and more oxidized states going down. Colors are Fe in rust, S in yellow, C in gray, Mo in magenta, and O in red. The unknown atom X at the center of FeMo-cofactor is shown in blue. The MoFe protein structure was prepared from PDB file 1M1N.pdb and the Fe protein was prepared from the PDB file 1FP6.pdb using the program PyMol.

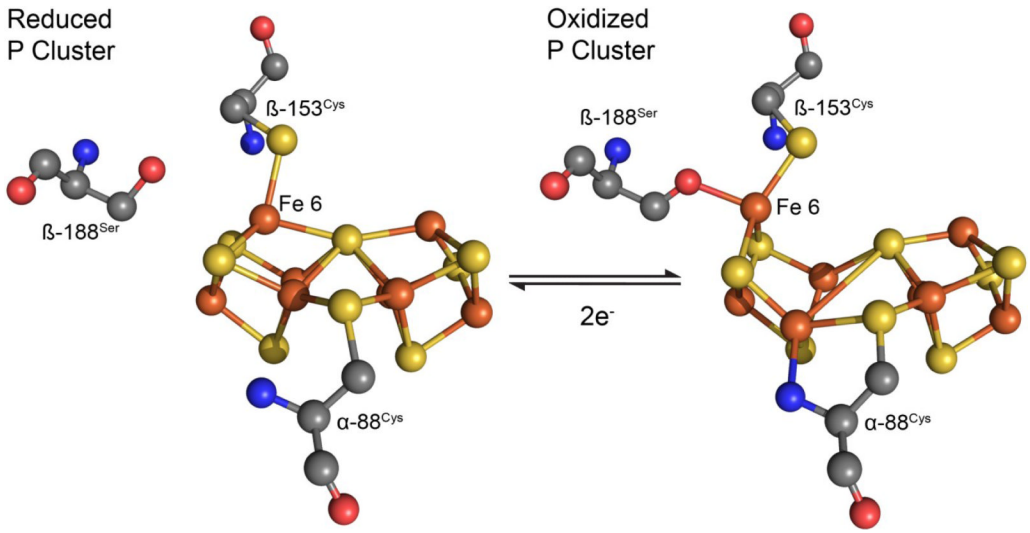

Figure 2. P-cluster in the oxidized and reduced states

Shown is the P-cluster in the reduced (P^N) state (left) and in the oxidized (P^{1+}) state (right) with the amino acids ß-153^{Cys}, ß-188^{Ser}, and α-88^{Cys} shown. Structures were generated from the PDB files 1M1N and 2MIN.

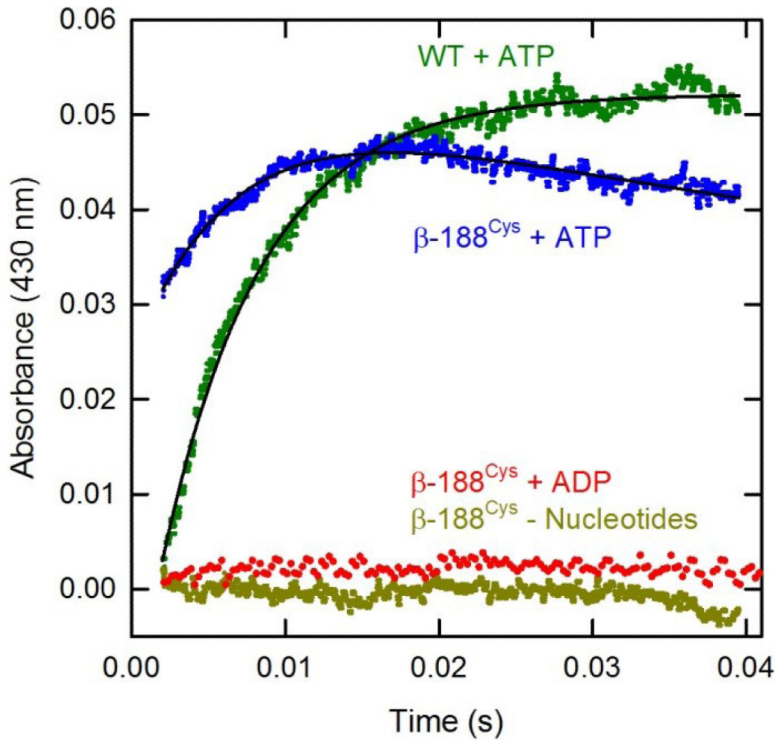

Figure 3. Electron transfer from the Fe protein to MoFe proteins monitored by stopped-flow spectroscopy

Shown is the absorbance at 430 nm plotted against the time after mixing Fe protein (75 μM) and MoFe proteins (20 μM) in one syringe against different solutions (without or with nucleotides at 18 mM). Shown is wild-type MoFe protein and Fe protein mixed with MgATP (WT+ ATP, green); ß-188^{Cys} MoFe protein and Fe protein mixed with MgATP (ß-188^{Cys} + ATP, blue); ß-188^{Cys} MoFe protein and Fe protein mixed with MgADP (ß-188^{Cys} + ADP, orange); and ß-188^{Cys} MoFe protein and Fe protein mixed with buffer without nucleotides (ß-188^{Cys} - nucleotides, light green). The top two sets of data were fit to a single exponential (solid lines) for the wild-type MoFe protein data and to a single exponential with a decline for the ß-188Cys MoFe protein data, with determined rate constants of 168 s^{-1} (WT+ATP) and 187 s^{-1} (ß-188^{Cys} + ATP). The mixing dead-time is ~ 2 ms. Other parameters and equations for fits are described in Materials and Methods.

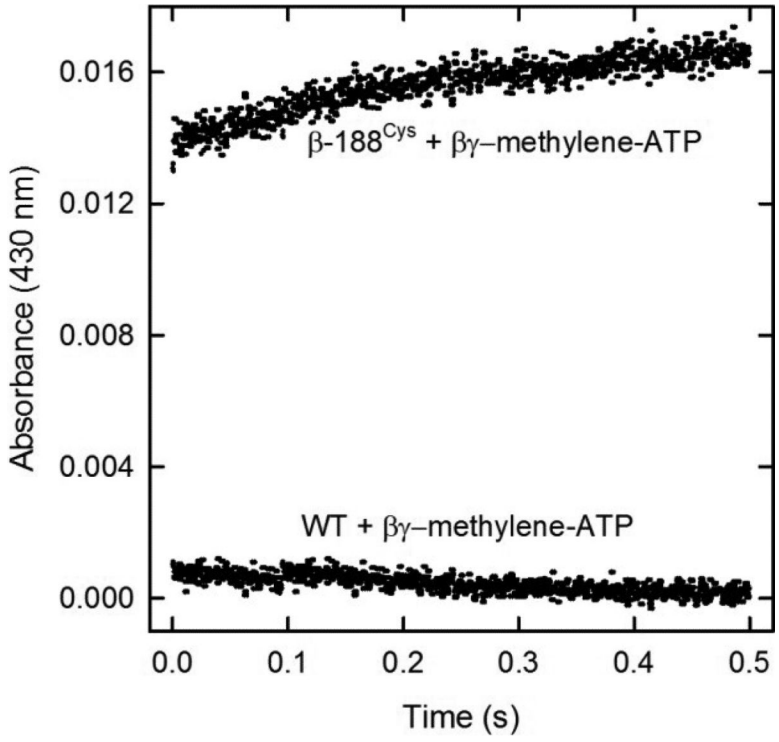

Figure 4. Electron transfer from Fe protein to MoFe proteins with the nucleotide analog αγ-methylene ATP

Shown is the absorbance at 430 nm plotted against the time after mixing Fe protein (75 μM) and MoFe proteins (20 μM) in one syringe with the nucleotide analog βγ-methylene-ATP (18 mM). Shown are β-188^{Cys} MoFe protein and Fe protein mixed against βγ-methylene-ATP (β-188^{Cys} + βγ-methylene-ATP); and wild-type MoFe protein and Fe protein mixed against βγ-methylene-ATP (WT + βγ-methylene-ATP).

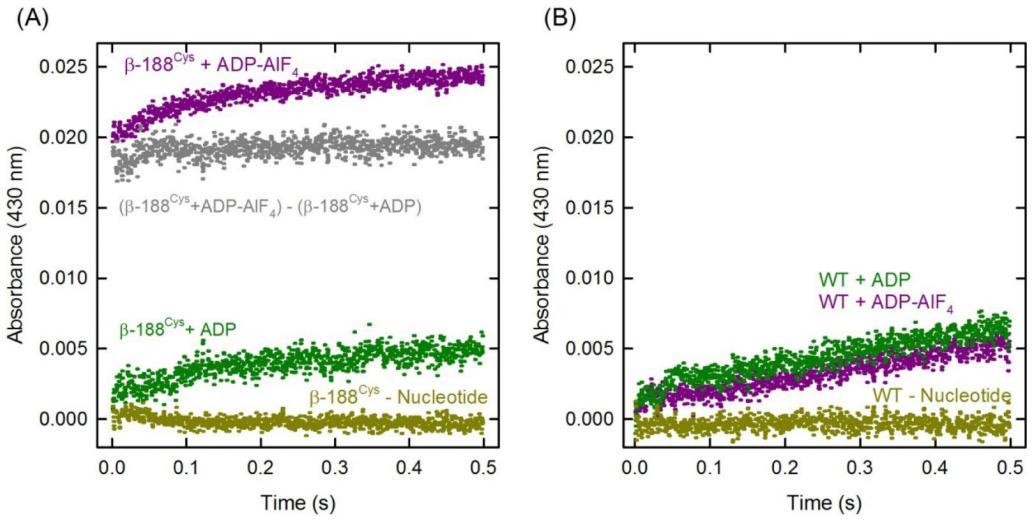

Figure 5. Electron transfer from Fe protein to MoFe proteins with the nucleotide analog MgADP-AlF_4^-

Shown is the absorbance at 430 nm plotted against the time after mixing MoFe protein (20 μM) and Fe protein (75 μM) with buffer (without or with nucleotide, 10 mM) in the stopped-flow. Shown in **panel A** is β-188^{Cys} MoFe protein and Fe protein mixed with $MgADPAlF_4^-$ (β-188^{Cys} + MgADP-AlF_4^-, purple); with MgADP (β-188^{Cys} + MgADP, green); without nucleotide (β-188^{Cys} - nucleotide, light green). Also shown is the difference spectrum ((ß-188^{Cys}+ADP-AlF_4) - (ß-188^{Cys} + ADP), grey). Shown in **panel B** is wild-type MoFe protein and Fe protein mixed with MgADP (WT + ADP, green); with ADP-AlF_4^- (WT + ADP-AlF4, purple); and without nucleotide (WT - nucleotide, light green).

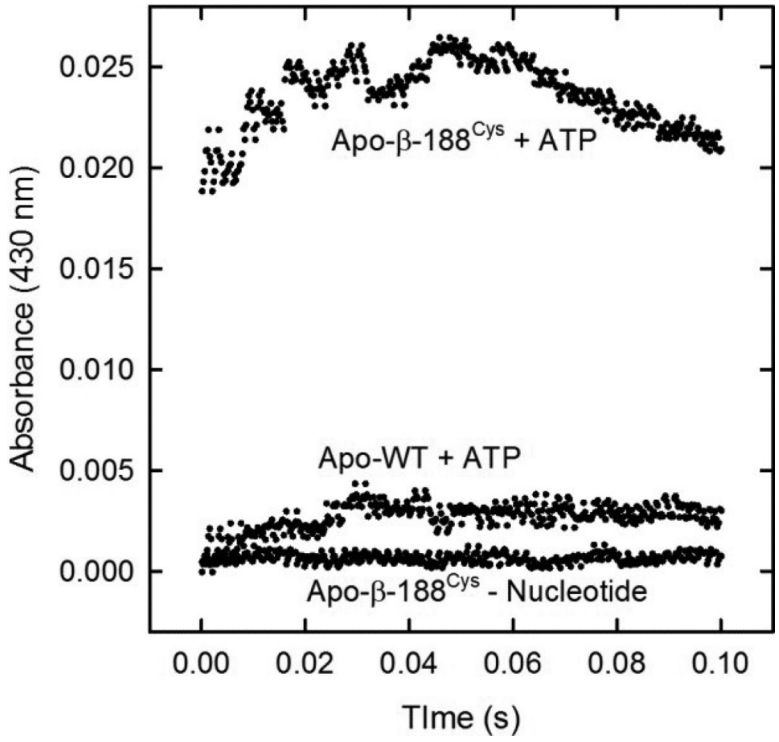

Figure 6. Electron transfer from Fe protein to apo-MoFe proteins

Shown is the absorbance at 430 nm plotted against the time after mixing Fe protein (75 μM) and MoFe protein (42 μM) with buffer (without or with nucleotides, 10 μM) in the stopped-flow. Shown are apo-ß-188^{Cys} MoFe and Fe protein mixed with MgATP (Apo-ß-188^{Cys} + ATP); apo-wild-type MoFe protein and Fe protein mixed with MgATP (Apo-WT + ATP); and apo-ß-188^{Cys} MoFe and Fe protein mixed with buffer lacking nucleotides (apo-ß-188^{Cys} - nucleotides). See the legend to Figure 3 for other details.

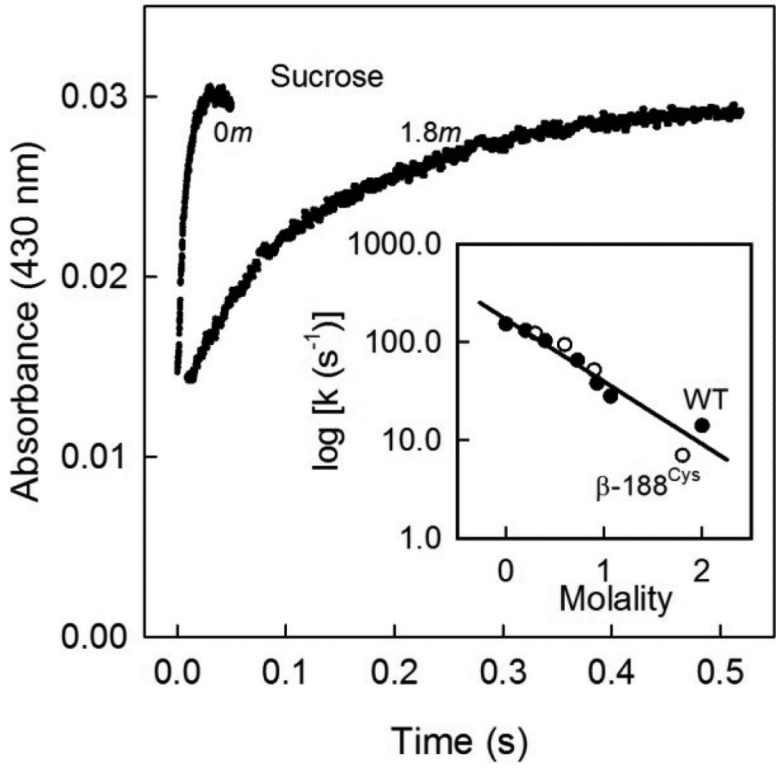

Figure 7. Osmotic pressure effects on electron transfer reactions from Fe protein to MoFe protein

Stopped-flow traces for ET from the Fe protein to the ß-188^{Cys} MoFe protein in the presence of 0, 0.6, 0.9 and 1.8 m sucrose (traces for 0 and 1.8 m sucrose are shown). The observed slow phases of the traces were fit to an exponential function to determine the rate constant (k_{obs}). (Inset) The log of the rate constants (k_{obs}) are plotted against the osmotic pressure of sucrose (m) for the ß-188^{Cys} (open circle) and wild-type (WT, closed circle) MoFe proteins and the points are collectively fit to a straight line.

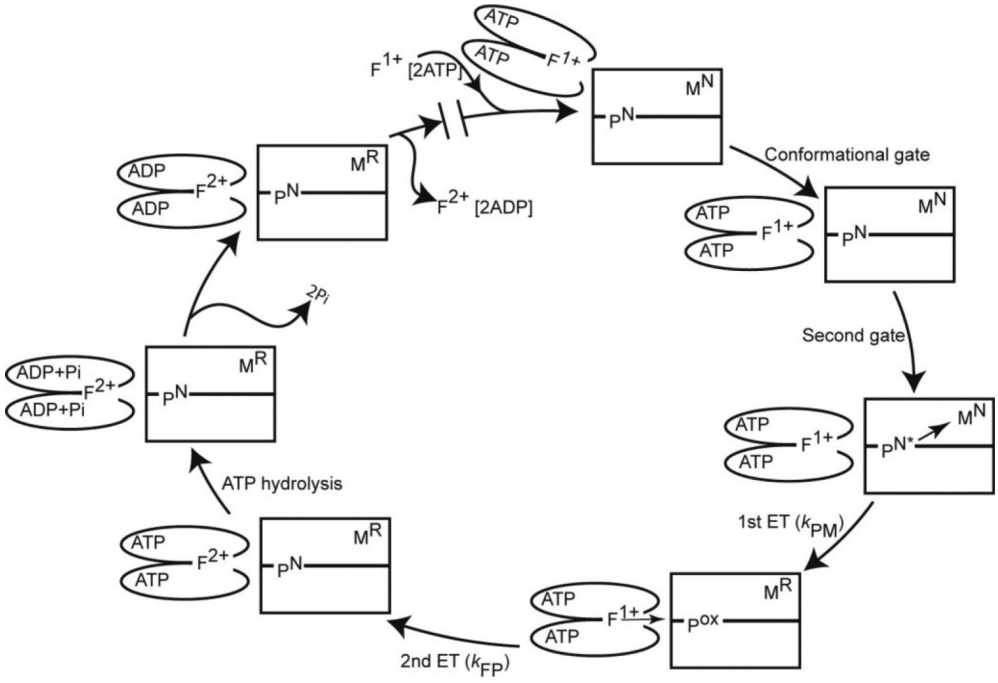

Figure 8. Models for nitrogenase mechanism

Shown is one catalytic cycle for a functional half of nitrogenase composed of an αß-unit of the MoFe protein (rectangles) and a homodimeric Fe protein (ovals) with the associated metal clusters: F = [4Fe-4S] in the 1+ or 2+ oxidation states, P = P cluster in the N or ox oxidation states, and M = FeMo-cofactor in the N or R oxidation states. The cycle starts at the top with reduced Fe protein +2 MgATP associating with the αß-unit of the MoFe protein (1). The remaining steps are numbered (clockwise): (2) the conformational gate, (3) the second gate, (4) the first ET (k_{PM}), (5) the backfill ET (k_{FP}), (6) ATP hydrolysis, (7) release of 2 Pi, (1) and replacement of oxidized Fe protein + 2MgADP with reduced Fe protein + 2MgATP.